Hindawi
Advances in Materials Science and Engineering
Volume 2022, Article ID 8907250, 10 pages
https://doi.org/10.1155/2022/8907250

Research Article

Mechanical Strengthening of Lightweight Aluminium Alloys through Friction Stir Process

P. Yogesh,[1] Santaji Krishna Shinde,[2] Shyamlal. C,[3] R. Suresh kumar,[4] Moti Lal Rinawa,[5] G. Puthilibai,[6] M. Sudhakar,[7] Kassu Negash,[8] and Rajesh S[9]

[1]*Department of Mechanical Engineering, Vel Tech Rangarajan Dr Sagunthala R and D Institute of Science and Technology, Avadi, Chennai 600062, Tamil Nadu, India*
[2]*Department of Computer Engineering, Vidya Pratishthan's Kamalnayan Bajaj Institute of Engineering & Technology, Baramati, Pune 413133, Maharashtra, India*
[3]*Department of Mechanical Engineering, Kalasalingam Academy of Research and Education, Krishnankovil, Tamil Nadu 626128, India*
[4]*Department of Mechanical Engineering, B. M. S. College of Engineering, Basavangudi, Bangalore 560019, Karnataka, India*
[5]*Department of Mechanical Engineering, Government Engineering College, Jhalawar 326023, Rajasthan, India*
[6]*Department of Chemistry, Sri Sairam Engineering College, Chennai 600044, Tamilnadu, India*
[7]*Department of Mechanical Engineering, Sri Sai Ram Engineering College, Chennai 600100, Tamil Nadu, India*
[8]*Department of Mechanical Engineering, Faculty of Manufacturing, Institute of Technology, Hawassa University, Hawassa, Ethiopia*
[9]*Department of Mechanical Engineering, Kalasalingam Academy of Research and Education, Krishnankoil, Tamil Nadu 626128, India*

Correspondence should be addressed to Kassu Negash; kassun@hu.edu.et

Received 11 December 2021; Revised 23 February 2022; Accepted 17 March 2022; Published 6 April 2022

Academic Editor: Chang Chuan Lee

The aerospace industries are focused on lightweighting with alloys having good tensile strength, fracture toughness, fatigue resistance, and corrosion resistance. The friction stir welding technology is one of the productive techniques in the aerospace industry to join such alloys with little ease. This paper deals with the composition of alloying elements that makes the structure lightweight and the impact of the precipitates evolved out of the selected alloying elements on the mechanical properties such as tensile strength and hardness of the joint in the aerospace alloys such as AA2xxx conventional aluminium alloys, AA2xxx lithium-based aluminium alloys, and AA7xxx aluminium alloys.

1. Introduction

The effective use of friction stir welding (FSW) technology, which is invented by TWI (The Welding Institute) [1–6], in the aerospace structures reduced the million number of rivets used in the aerospace structures that resulted in better joint tightness and reduced vibration along with reduction of several kilograms of weight. In addition to the above, by providing a leak proof joint, this welding technique improves the mechanical properties of the end product. The finer grains produced by FSW technique withstands heavy impact and is tough enough to handle heavy loads (very useful for ballistic applications). The welding parameters such as rotation speed (N) (*heating effect*), traversing speed (V) (*cooling effect*), the distribution of coherent precipitates (including sheared precipitates), and wt.% of alloying elements play a major role in deciding the hardness and tensile strength in the weld joint. In FSW, strengthening mechanism can be divided as precipitation strengthening (more pronounced in base metal (BM)), solid solution strengthening, dislocation strengthening, and fine grain strengthening (particularly in stir zone (SZ)).

However, the precipitate formation, temper selected, and dislocation hindrance are considered to be the major mechanisms to increase the strength of the joint and base material. At the outset, the equiaxed grains in the stir zone (SZ) impedes more dislocations by the increased grain boundary area. Hence, the synergetic effect of precipitate formation (less influence) [7] and equiaxed grains (more grain boundary area and higher influence) in the stir zone and thermo-mechanically affected zone make FSW joint efficiency superior than fusion welding and other allied welding processes. FSW joint efficiency is defined by the hardness in the weakest area of the weld commonly referred as low hardness distribution region (LHDR). The LHDR may be either in the heat affected zone (HAZ) (*W hardness distribution*), at the interface between HAZ and thermo-mechanically affected zone (TMAZ) (*W hardness distribution*), or even at stir zone (*V hardness distribution*), as discussed by Mishra et al. [8]. The LHDR is decided by the density of precipitates and the density of dislocations and the heterogeneous nucleation of precipitates in the dislocations. Hence, the precipitates and dislocations play a major role in increasing the hardness of the structure [9, 10]. When the speed is increased, from low rpm to high rpm, the precipitates grow, which led to its dissolution in the stir zone that in turn leads to decreasing trend in the hardness in the stir zone [11]. Further, Yadav et al. [12] discussed about the rotational speed of the tool. It was observed that the disappearance of hard precipitates during friction stir welding in the stir zone and reappearance of the hardened precipitate (Al-Cu) in the stir zone after PWHT while welding AA2024 - T3. The disappearance of the precipitate is due to the higher rotational speed of the tool. The reformation of precipitates is also influenced by the alloying elements present, the aging time, and temperature. The base metal mechanical properties (*tensile strength*, *hardness*, *fracture toughness*, *fatigue resistance*) are considered as the important parameters for end use.

Furthermore, the addition of alloying elements enhances the strength, corrosion, and ductility of the parent metal. For example, the addition of lithium to aluminium enhances the elastic modulus of the material and also decreased the density of the metal, which is used in aerospace application. A minor addition of scandium (Sc) resulted in major increase in the strength of the order of 50 to 100 MPa per 0.1 wt. % due to Al_3Sc dispersoids as told by Sauvage et al. [13]. The addition of scandium in the aluminium matrix restricts the grain growth and stops the movement of grain boundary. In addition to that, vacancies play a crucial role in developing and maintaining the strength of the metal. The vacancies are responsible for the enhanced diffusion of atoms of alloying elements. For example, face-centered cubic structure (FCC) has more vacancy creating structure than body-centered cubic structure (BCC). Hence, the solute atoms will be absorbed more easily in FCC than in BCC. During rotation of the tool, in the case of AA2024 alloy where Cu is more (up to 4.5%), a large number of precipitates will be broken up (more intermetallic Al_2Cu–BCT structure) and block the movement of dislocations, which increase the hardness and tensile strength of the workpiece. Conversely, the coarsening of the precipitates may induce ductility of the joint in some cases. Hence, the shape of the precipitates and its density influence the hardness of the joint. The needle-shaped precipitates are coherent with matrix than rod-shaped precipitates. Hence, mechanical properties depend on the density of the needle-shaped precipitates as told by Sato et al. (AA6063-T5) [14]. Moreover, the temper of the material also increases the base metal hardness. When the base metal has more hardness, eventually, the joint also exhibits better efficiency. The tool breaks the precipitates and nucleates more precipitates, which act as barriers for dislocation motion thereby increasing the hardness and tensile strength. Further, if the difference between ultimate tensile strength and yield strength value is more for an alloy, then it can be said that the crack tolerance will be good for the particular structure. Initially, this technology was adopted to weld light metals such as monolithic aluminium and magnesium alloys. But after the invention of Al-Li alloy series, this technology has been adopted as a unique technique for joining aerospace alloys. Also, aluminium alloys are considered as the chief alternative [15] to steel in automobile industries because of its better specific strength, better specific stiffness, and its better corrosion resistance [16, 17]. Moreover, the low density of aluminium alloys makes it the suitable candidate for designing complex products than steel allowing better design freedom and also allows designers to build structures with more thickness (more safety in case of accidents in automobiles than steels due to excellent ductility). The addition of aluminium alloy in the aerospace industry leads to the reduction in emission by reducing the weight of the airplane. Particularly, the lithium-based aluminium alloys are the preferable candidate alloy for the above purpose of lightweighting. The lithium-based aluminium alloys have been invented to replace the AA7xxx and AA2xxx aluminium alloys to offer more strength, stiffness, and elongation than conventional aluminium alloys. But there exists a disadvantage in lithium-based aluminium alloys that is anisotropy behavior and the formation of coherent but shearable Al_3Li precipitate. In order to mitigate this effect, Cu and Mg are added in these alloys for the formation of precipitates such as Al_2CuLi and Al_2CuMg. These precipitates increase the hardness, tensile strength, and fracture toughness of the aerospace structure (for example, cryogenic fuel tank in rockets) but with reduced density to achieve better specific stiffness. These lithium-based aluminium alloys are used as the replacement of AA2024 and AA7075 alloy in the aerospace industry.

This paper deals with the tensile strength and hardness of the lightweight aerospace alloys such as AA2050, AA2060, AA2198, AA7475, AA7050, AA7055, AA2024, and AA7075. The aforementioned properties are essential for aerospace alloys to prevent crack propagation in higher altitudes.

2. Types of Precipitation Hardening Aluminium Alloys and Their Tempers

2.1. Types of Precipitation Hardening Aluminium Alloys and Their Precipitates. This subsection deals with types of

precipitation hardening aluminium alloys. Generally, the temper designation refers to the degree of hardness of the aluminium alloy material. The aging time also influences the hardness of the aluminium alloys. The aluminium alloys that belong to the above category are AA2xxx, AA6xxx, and AA7xxx alloys. In AA2xxx alloys, the major alloying element is copper (Cu), which increases the tensile strength of the component but retard corrosion resistance; Li is another alloying element that forms the precipitate Al_3Li (a coherent precipitate); it also forms other type of precipitates with Cu and Mg such as Al_2CuLi and Al_2CuMg to enhance tensile strength and increase elongation. In AA6xxx alloys, the major alloying elements are magnesium and silicon (Mg and Si). The Mg adds strengthening effect to the alloy; it also increases micro hardness of the alloy due to HCP crystal structure and Si induces fluidity for the alloy. The precipitate formed by Mg and Si is -Mg_2Si having FCC crystal structure. In AA7xxx alloys, the major alloying elements are magnesium and zinc (Mg and Zn). The precipitate formed between Mg and Zn is $MgZn_2$ (magnesium di zinc) and Al_3Zr (*a dispersoid*) having HCP crystal structure (*6 atoms per unit cell*), which impart better hardness than FCC structure (*4 atoms per unit cell*). In all the above-said alloys, Fe is an insoluble impurity that must be controlled to avoid brittle fracture, which initiates in the grain boundary.

2.2. Temper Designations Applicable for Aerospace Alloys. This subsection analyses the temper designations applicable for aerospace alloys. During solutionizing, single solid solution comprising primarily aluminium and solute forms either as substitutional or interstitial in solution state. After solutionizing, the metal will be quenched to a room temperature. When the solvus line is touched in the phase diagram and during aging much below the solvus line, guinier preston zones are generated. At this stage, vacancies created above the solvus line will be supersaturated in room temperature. The aging performed after quenching accelerates the diffusion of atoms in the generated vacancies and vacancy loops to produce strong and ductile structure. Moreover, the tensile strength and hardness of the base metal for the joint will change based on the temper as discussed by Chen et al. [18]. The selection of the temper is based on the application of the material. For example, A class surfaces can be produced in automobiles using the aluminium alloy having T651 temper and for better corrosion resistance, peak-aged temper (T7, T87) will be chosen. The following subsection deals with the types of tempers used in industries.

2.2.1. Underaging Tempers

T3. Solution heat treatment, cold work, and natural aging. It is used for the aerospace alloy AA2024.

T6. The O tempered aluminium billet is heated to about 990°F and then quenched in water followed by aging at about 350°F for around 8 hours. This temper will increase the yield strength of the base material. This temper is used with AA6061 aluminium alloy. This temper designation is for artificial aging. This temper can be used to achieve better flatness. Solution is heat treated and artificially aged to attain maximum strength.

T651. In this temper along with T6 treatment, 1% to 3% straightening is done to relieve the residual stresses and to increase the dislocations. This temper is a very stable temper.

2.2.2. Peak-Aging Tempers

T7. Better crash resistance. Slightly decreased strength and improved ductility. This temper is used to achieve better dimensional stability. But this temper will consume other small precipitates leading to decrease in strength of the alloy. This temper also increases corrosion resistance but degrade mechanical properties as suggested by Pagalia et al. [19].

T7451. This temper is used along with AA7050 for aerospace applications. It combines high strength with good exfoliation corrosion resistance and average stress corrosion cracking resistance.

T76. It provides highest strength with exfoliation corrosion resistance and stress corrosion cracking resistance.

T7651. It provides better exfoliation corrosion resistance and stress corrosion resistance with average strength.

T8. Solution heat treated, cold worked, then artificially aged. The cold working increases the number of dislocations that aid for heterogeneous nucleation of precipitates and hence better mechanical properties will be obtained. This temper is used for AA2050 and AA2060 aluminium lithium alloy.

T87. This is one of the standard temper for AA8090 alloy, 7% cold work (by rolling and stretching) with age hardening to increase the dislocations and to produce flatness. Solution treatment with water quenching, 7% cold work and peak aging. This temper is used for AA8090 aluminium lithium alloy.

3. Overview of Precipitation

Generally, the precipitate evolution is the desirable phenomenon in aluminium alloys. Precipitation is favored by the process of artificial aging. In precipitation hardening alloys, the precipitation sequence occurs as Θ" (GP zones-coherent) ⟶ Θ' (semicoherent) ⟶ Θ (stable precipitate) ⟶ precipitate coarsening (over-aging) [20–22]. Θ" are the cluster of precipitates of few tens of nm size, Θ′ are the precipitates of few hundreds of nm size (larger size than Θ") and Θ is the stable size of the precipitate (larger than previous two versions of precipitates) and beyond the stable size, more precipitate coarsening (phenomenon of overaging) occurs which led to the decrease in hardness in the stir zone (SZ) when the temperature favors for the growth of the precipitate. The precipitates are of three

type's, namely, Coherent, semi coherent and incoherent. During the formation of precipitate, coherency with *a* solution (aluminium and solute component) is very important. The coherent precipitate will slowly change to semi-coherent precipitate when the precipitate grows (lessening of fine precipitates start). The coherent precipitate (*quasi-unstable*) will have higher strain energy. In the stage of semi coherency, the dislocation will start to form when the temperature is further increased, the semi coherent precipitate *(metastable*) changes to very few large incoherent precipitate (*stable*). The incoherent precipitate is defined as stable precipitate [23] due to the extra ordinary growth which will consume small finer precipitate as suggested by Anderson et al. [24]. During the transition from coherent to incoherent precipitation, the maximum hardness and tensile strength will be attained. Hence, more number of coherent and incoherent precipitate induces better hardness than incoherent precipitate. The precipitate is grown to the specified size and composition (morphology).

If the precipitate is larger, the dislocation adopts the looping mechanism (Orowan strengthening mechanism) [25, 26] to by-pass large precipitate. The hardness will be better in the stage of coherency. There is a relation between precipitates and dislocation initiation. The semi coherent precipitates introduce dislocation in the matrix due to elastic straining around the precipitate (solute). Grain boundaries also play a significant role in increasing the strength of the alloy. When the grain boundary restricts the movement of dislocations, it increases the strength of the structure. If the dislocations are introduced in the grain boundary (heterogeneous nucleation), the yield strength decreases. There is also a possibility of precipitate-free zones (PFZ's) near the grain boundary where hardness is very lesser. The PFZ is created due to the large size of precipitates consuming equiaxed or small precipitates near grain boundary making the vicinity of grain boundary completely free of precipitates. The hardness is a main concern when dislocations nucleate at precipitate free zone (PFZ). This will decrease the yield strength makes the area prone to failure as discussed by Thorsten Krol et al. [27]. Liu et al. [28] detailed about the formation of different size of precipitates and its influence on hardness and microstructure. It is told that the base metal and heat affected zone (HAZ) has similar density of dislocations. After the workpiece is placed in welding fixture, there will be no cold work or plastic deformation takes place in the base metal and in the HAZ. The deformation takes place only in the stir zone creating more number of equiaxed grains thereby enhancing the strength of the joint. But, HAZ receives strength only from solution treatment and aging. Hence, it is told that stir zone exhibits higher hardness than HAZ [29–31].

It is also understood that whenever the tool rotation speed increases, the precipitate size is increased due to the change of coherent to stable precipitate. The stable precipitate has little influence in increasing the hardness in the joint and elsewhere in the workpiece. The coherency will be lost when precipitates begin to grow due to temperature increase. In the stir zone, more temperature is created near to solidus temperature. Hence, more number of undissolved precipitates will reappear in the stir zone.

3.1. Possible Combination of Precipitates. The major alloying elements added in the aluminium series are copper (Cu), magnesium (Mg), manganese (Mn), silicon (Si), zinc (Zn), titanium (Ti), and lithium (Li) (*aerospace*). In general, the precipitates formed are Al_2Cu (a precipitate of aluminium and copper but rich in aluminium in the aluminium side of binary phase diagram-FCC structure), Mg_2Si (magnesium silicide rich in magnesium), and $MgZn_2$ (di zinc magnesium rich in Zn-HCP structure). Zn and Cu are added to aluminium alloys to increase the strength along with Al, but it will reduce the ductility. Si (*an impurity*) is added to the alloy to increase the fluidity of the alloy. Si with Mg produces the intermetallic compound that has better mechanical properties. Ti is added to the alloy as the grain refiner. Zr is added to the alloy to produce fine precipitates and forms precipitate with aluminium-Al_3Zr, which has the role of restricting the movement of grain boundary. Fe and Si are impurities in the alloy. Ni is added to enhance the high temperature strength. Li is added to the alloy to enhance the ductility (*through modulus of elasticity*) and to reduce the density of the alloy. As lithium is expensive than other alloying elements, it is extensively used only in aerospace applications. The main aim of adding Li is to reduce the density of aluminium making the aircraft fuel efficient [32]. The final aim of the heat treatment procedure (*artificial aging*) that starts from the base metal temper to postweld heat treatment (PWHT) of FSWed alloy is to achieve fine precipitates to attain sufficient tensile strength to resist deformation and fracture in the stir zone and in other zones of the weld.

3.2. Morphology of Precipitates. The precipitates take the shape of sphere (*coherent precipitate*) to plate and disc morphology (semi-coherent/incoherent precipitate). The spherical GP zones (*precipitate zones*) will be formed, whenever the atom size between the matrix and solute is the same. The GP zones will deviate from the spherical shape (*disk shape*) when the atoms of matrix and solute are of different sizes [33]. The shape of the precipitates is governed by Gibb's free energy, G, and is given as

$$\begin{aligned} G &= H - TS, \\ H &= U + PV, \\ H &\approx U. \end{aligned} \tag{1}$$

Here, P = pressure, bar, and V = volume, m^3.

In precipitation, after FSW internal energy, U (may be responsible for internal stress generation) dominates the enthalpy, H. Hence, Gibb's free energy is directly proportional to internal energy. The term TS (combined effect of temperature, T and entropy, S) can be neglected as friction stir welding is a solid state welding process (disorderliness of atoms is lesser). Hence, Gibbs free energy equals internal energy. When atoms start to vibrate, it expands the grain boundary. Lowest free energy ($\Delta G < 0$) is the state of thermal

equilibrium that leads to in-coherency [34] in precipitation development. The spontaneous reaction (*natural reaction*) takes place from coherent to incoherent phase. Many elements inside the alloy show metastable (semi-coherent) phases that are compounds formed along with the matrix (Al) and also with other alloying elements being added.

Generally, it is assumed that the matrix phase is infinite phase and the precipitate phase is finite phase. The basic concept behind the changing shape of precipitates is the agglomeration (accumulation) of solute atoms (Figures 1 and 2) in the combined form. Initially, the precipitate will be in the form of a sphere. When the solute atoms start to accumulate, then the shape changes to disc and plate shape thereby becoming incoherent having lowest strain energy up on experiencing heat. The morphology of the precipitate changes from sphere to plates or disks depends on the temperature involved. The sphere morphology [10, 35, 36] (GP zones at room temperature) is an unstable morphology. Hence, the precipitate grows until it attains stable morphology (lower strain energy). The precipitates also nucleate and grow when the dislocations shear the precipitate.

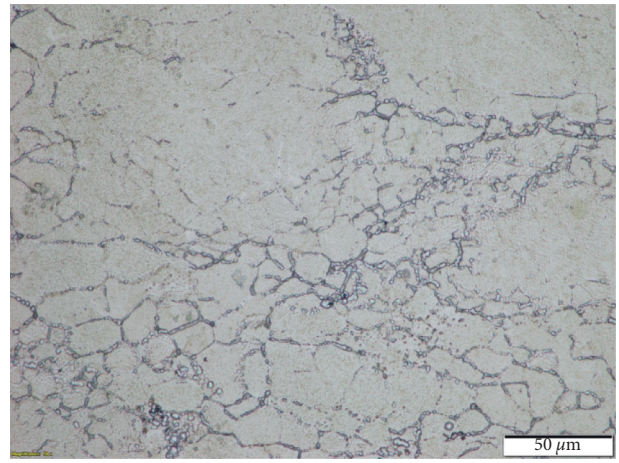

Figure 1: SEM image of aluminium series alloy indicating the accumulation of atoms as grain boundary.

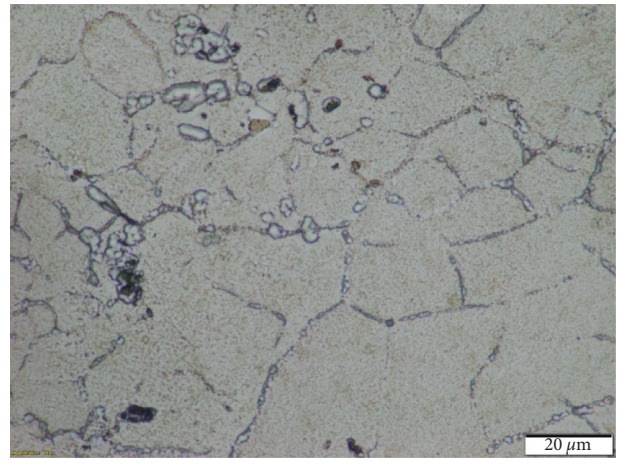

Figure 2: The etched marks in the grain boundary (enlarged view).

4. Influence of Chemical Composition on the Precipitate Formation and Its Effect on Mechanical Properties

Figure 3 and Table 1 present the chemical composition of alloys that is recommended for lightweight applications in aerospace industry such as AA2024, AA2060, and AA7075. From the above table, it can be clearly seen that Cu, Mg, Zn, and Li have more wt. % elements. In the above-mentioned alloys, the Li-based aluminium alloy has been invented to replace the conventionally used AA2xxx and AA7xxx series alloys. Cu and Mg are intentionally added to Li-based alloys to the formation of S phase (Al_2CuMg) and T1 phase (Al_2CuLi). These element additions will reduce the anisotropy and increases the elongation of the alloy and also impart better properties. Compared to a conventional alloy, every 1% lithium presence increases the elastic modulus by 3%, while decreasing the density by 6%. It is a quaternary alloy capable of ensuring, in addition to the aforesaid form and density effects, a high response to aging treatment, thanks to the formation of the metastable phase δ' (Al_3Li) coherent with the matrix and other magnesium and copper phases. Zirconium presence allows it to control the grain structure and also plays a beneficial nucleating effect on the δ' particles.

Hence, the intermetallic precipitates will be more involving Cu, Mg, Zn, and Li. In Li-based alloys to impart ductility to the alloy, which is clearly indicated in Cu/Li ratio. Also Mg is intentionally added to other alloys as an alloying element to increase the hardness of the alloy, since it has HCP structure. In the above-mentioned alloys, Cu dominates Mg except for AA7xxx series where Mg dominates Cu, which is clearly indicated in the above table. Cu is added to aluminium alloy to increase tensile strength by forming precipitates such as Al_2Cu, Al2CuLi, and Al2CuMg, which will precipitate up on reaching the solvus line in the Al-Cu phase diagram and fatigue strength to AA2xxx alloy and Zn is added to AA7xxx alloys along with magnesium and copper to form $MgZn_2$ precipitate. Generally, Zn, Cu, and Mg are added to influence natural aging and artificial aging. In AA2060 alloy, Zr (0.1%) is intentionally added to increase the dispersoids (Al_3Zr), which will strengthen the grain boundary and to inhibit recrystallization as told by Xie et al. [45]. In all the above-mentioned compositions, Ti (trace element) was added to intentionally control the grain size (to approach finer size) by forming Al_3Ti compound. Hence, the precipitates involving Zn, Cu, Mg, and Li content will appear as the precipitate after aging treatment as mentioned in Figure 3.

In Figure 4, two types of temper are presented, namely, T6-underaged temper and T7 and T8-peak-aged temper. Both types of temper are used in aerospace industries. It is observed that the strength of 2024 is lesser than 7075. In 7075, $MgZn_2$ exhibits HCP structure (*fewer slip systems*), but in 2024, Al_2Cu exhibits FCC structure (Figure 5) (*more slip systems*). In HCP structure, deformation takes place by twinning that makes the material stronger than AA2xxx category. In AA7075, in addition to Cu, Zn is also

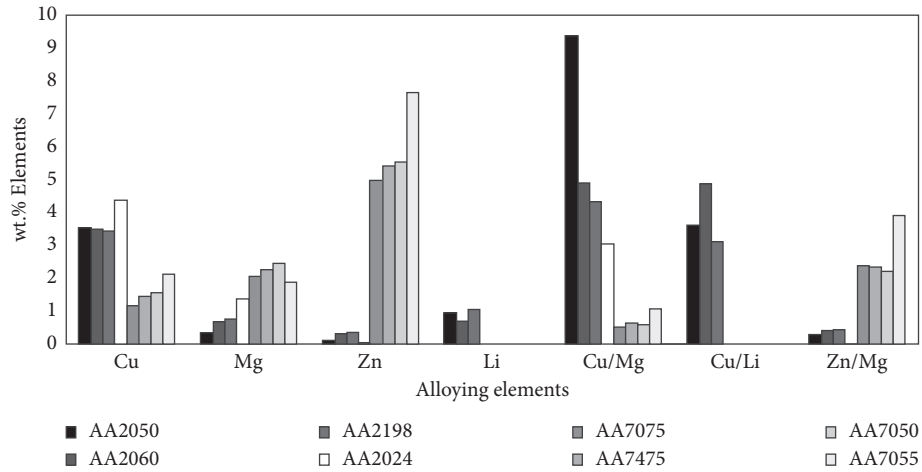

Figure 3: Bar diagram of chemical composition of aerospace alloys [37–44].

Table 1: Chemical composition of aerospace alloys.

Alloy	Cu	Mg	Zn	Li	Cu/Mg	Cu/Li	Zn/Mg
AA2050	3.6	0.38	0.12	0.98	9.47	3.67	0.32
AA2060	3.56	0.72	0.34	0.72	4.94	4.94	0.47
AA2198	3.5	0.8	0.35	1.1	4.38	3.18	0.44
AA2024	4.43	1.42	0.06	0	3.12	0.000	0.04
AA7075	1.2	2.1	5.1	0	0.57	0.00	2.43
AA7475	1.5	2.3	5.5	0	0.65	0.00	2.39
AA7050	1.6	2.5	5.6	0	0.64	0.00	2.24
AA7055	2.18	1.95	7.72	0	1.12	0.00	3.96

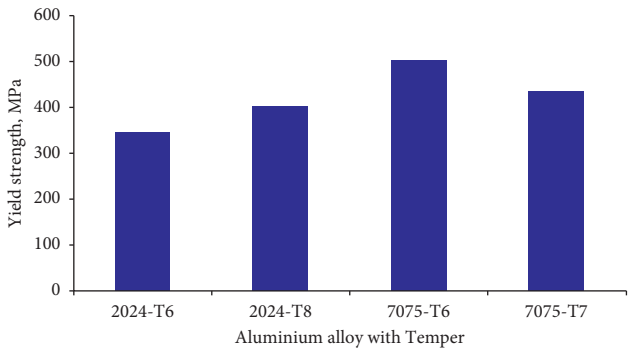

Figure 4: Yield strength of precipitation hardening aluminium alloys.

present that also contribute to increase in the strength of the alloy as told by Ipekoglu et al. [46] Further, Zinc dissolves more in aluminium during solution stage and make the material stronger that reappear at room temperature creating more number of precipitates, which makes the material suitable for high-temperature applications.

From Figure 6, it is ascertained that Cu content in AA2024 aluminium alloy produces higher tensile strength and hence hardness. The coarse precipitates in AA7075 with T7 temper and in AA2024 with T8 temper produce lesser hardness than AA7075 with T6 temper due to the absence of solid solution hardening and the disappearance of

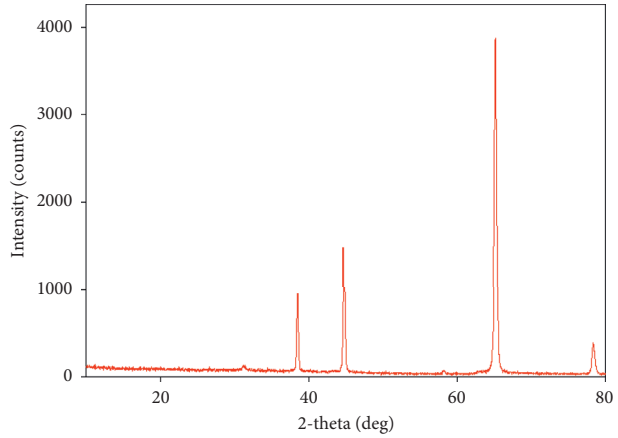

Figure 5: XRD spectrum of aluminium alloys: AA2xxx and AA7xxx alloys.

precipitates. But, hardness can be recovered to some extent using PWHT as suggested by El. Danaf and El-Rayes [47].

Figure 7 indicates hardness of the FSW joint that is 140 VHN for AA7075 T7, which is 87.5% of the base metal hardness [19], and 123 VHN for AA7075 T6 [48], which is 68.33% of the base metal hardness. The reason for the decrease in hardness in AA7075 T6 compared to the base metal is due to the presence of dynamic recrystallization [49–52] in the stir zone that might have fragmented [53] many incoherent precipitates to coherent precipitate that allow more dislocation to pass through and also reduces dislocation density.

Figure 8 displays the base metal with tempers. In the peak-aged temper (T7, T8), the elongation at break increased compared to its underaged temper before processing in friction stir welding due to more number of coarsened stable precipitates. As coarsening of precipitates induces ductility, elongation at break % is higher for peak-aged tempers but can be reduced by PWHT (postweld heat treatment) as suggested by Sivaraj et al. [54].

Cabrini et al. [48] investigated the SEM of FSW joint and found that wt. % Zn (8.4%) is rich in pct, as compared to Cu

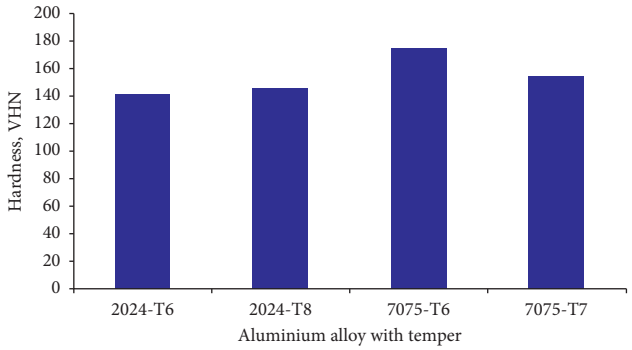

Figure 6: Vickers hardness of precipitation hardening aluminium alloys.

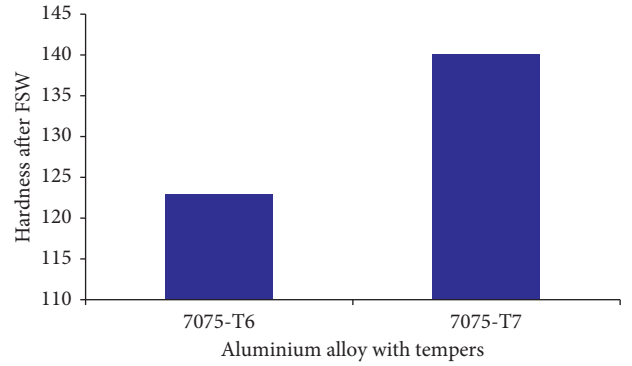

Figure 7: Hardness of aluminium alloys after FSW.

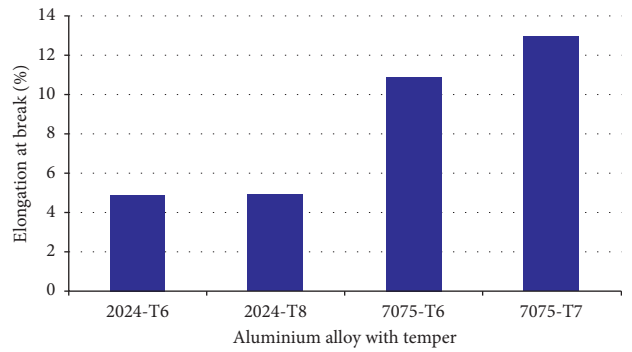

Figure 8: Ductility chart for precipitation hardening aluminium alloys.

and Mg due to the fact that Zn dissolves more in aluminium than other two elements mentioned above in the solutionizing stage. Hence, coherent $MgZn_2$ precipitate is developed inside the grain and in the grain boundaries due to dynamic recrystallization. When compared with base metal AA7075-T6 composition (Figure 1), Wt. % Zn 8.48 is in upper hand that introduces better strength to the joint. As seen from Figure 9, Zn has more atoms than Mg and Cu. Hence, the hardness value of 124 VHN compared to base metal hardness of 180 VHN as seen from Figure 7 is appreciable. This hardness is attained due to the precipitation of $MgZn_2$ and equi-axed fine grain structure after FSW in the weld joint. Hao et al. [55] discussed about the precipitation behavior of AA7075-T6

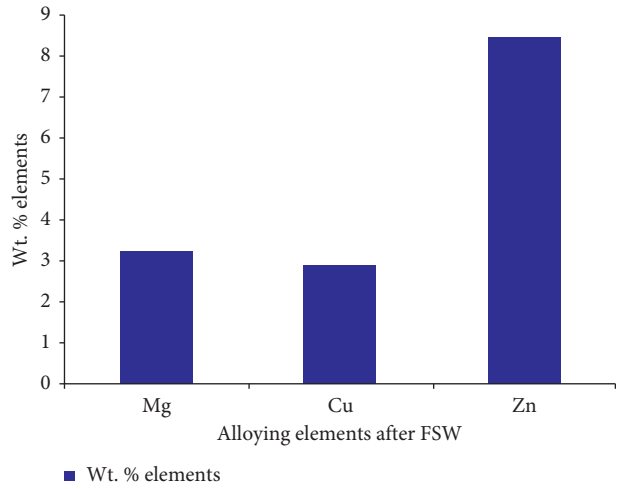

Figure 9: Wt. % elements after FSW as proposed by Cabrini et al. [48].

alloy with 6 mm thickness. It was found that the distribution of precipitates varied with rotational speed. It was found that the strengthening to the weld zone was provided by strain hardening effect and Cu-containing precipitate, which is in agreement with Behzadi et al. [56] and Xu et al. [57]. Furthermore, Hernandez et al. [58] discussed about the ratio of Cu and Mg in AA2024 alloy. Combined effects of chemical composition and plastic deformation influence strengthening behavior and precipitate mechanism. It was suggested that strength can be increased by solid solution, strain hardening, and precipitate hardening. Hardness is influenced mainly by precipitation formation but is modified by plastic deformation and Cu/Mg ratio.

5. Conclusions

In this work, mechanical properties such as tensile strength and hardness of the alloy in the context of alloying elements present in the alloy are covered in greater detail. The following observations were made:

(i) The importance of alloying elements and its contribution in the precipitate formation that led to the improvement in mechanical properties has been discussed

(ii) Mechanical properties such as tensile strength and hardness of the alloy have been discussed

(iii) The significance of temper in improving the mechanical properties has also been discussed

(iv) The effect of free energy of the system in the precipitate growth has been briefed

(v) The contribution of welding parameters in improving the mechanical properties of the stir zone has been detailed

Abbreviations

U: Internal energy, J
H: Enthalpy, J/Kg

P: Pressure, bar
V: Volume, m^3
T: Temperature, deg. Celsius
S: Entropy, J/K
GP: Guinier preston zones
BCC: Body-centered cubic structure
FCC: Face-centered cubic structure
HCP: Hexagonal close packed structure.

Data Availability

The data used to support the findings of this study are included in the article. Should further data or information be required, they will be available from the corresponding author upon request.

Disclosure

It was performed as a part of the Employment Hawassa University, Ethiopia.

Conflicts of Interest

The authors declare that there are no conflicts of interest regarding the publication of this paper.

Acknowledgments

The authors appreciate the technical assistance to complete this experimental work from Department of Mechanical Engineering, Sri Sai Ram Engineering College, Chennai 600100, Tamil Nadu, India.

References

[1] W. He, M. Li, Q. Song, J. Liu, and W. Hu, "Efficacy of external stationary shoulder for controlling residual stress and distortion in friction stir welding," *Transactions of the Indian Institute of Metals*, vol. 72, no. 5, pp. 1349–1359, 2019.

[2] G. Singh, K. Singh, and J. Singh, "Effect of process parameters on microstructure and mechanical properties in friction stir welding of aluminum alloy," *Transactions of the Indian Institute of Metals*, vol. 64, no. 4-5, pp. 325–330, 2011.

[3] C. Devanathan and A. S. Babu, "Friction stir welding of metal matrix composite using coated tool," *Procedia Materials Science*, vol. 6, pp. 1470–1475, 2014.

[4] M. M. Attallah and H. G. Salem, "Friction stir welding parameters: a tool for controlling abnormal grain growth during subsequent heat treatment," *Materials Science and Engineering*, vol. 391, no. 1-2, pp. 51–59, 2005.

[5] G. M. F. Essa, H. M. Zakria, T. S. Mahmoud, and T. A. Khalifa, "Microstructure examination and microhardness of friction stir welded joint of (AA7020-O) after PWHT," *HBRC Journal*, vol. 14, no. 1, pp. 22–28, 2018.

[6] P. Xue, B. L. Xiao, D. R. Ni, and Z. Y. Ma, "Enhanced mechanical properties of friction stir welded dissimilar Al-Cu joint by intermetallic compounds," *Materials Science and Engineering*, vol. 527, no. 21-22, pp. 5723–5727, 2010.

[7] R. K. R. Singh, C. Sharma, D. K. Dwivedi, N. K. Mehta, and P. Kumar, "The microstructure and mechanical properties of friction stir welded Al-Zn-Mg alloy in as welded and heat treated conditions," *Materials & Design*, vol. 32, no. 2, pp. 682–687, 2011.

[8] P. S. De and R. S. Mishra, "Friction stir welding of precipitation strengthened aluminium alloys: scope and challenges," *Science and Technology of Welding & Joining*, vol. 16, no. 4, pp. 343–347, 2011.

[9] M. M. Moradi, H. Jamshidi Aval, R. Jamaati, S. Amirkhanlou, and S. Ji, "Microstructure and texture evolution of friction stir welded dissimilar aluminum alloys: AA2024 and AA6061," *Journal of Manufacturing Processes*, vol. 32, pp. 1–10, 2018.

[10] O. Gopkalo, X. Liu, F. Long, M. Booth, A. P. Gerlich, and B. J. Diak, "Non-isothermal thermal cycle process model for predicting post-weld hardness in friction stir welding of dissimilar age-hardenable aluminum alloys," *Materials Science and Engineering*, vol. 754, pp. 205–215, 2019.

[11] P. Vijaya Kumar, G. Madhusudhan Reddy, and K. Srinivasa Rao, "Microstructure and pitting corrosion of armor grade AA7075 aluminum alloy friction stir weld nugget zone - effect of post weld heat treatment and addition of boron carbide," *Defence Technology*, vol. 11, pp. 166–173, 2015.

[12] V. K. Yadav, V. Gaur, and I. V. Singh, "Effect of post-weld heat treatment on mechanical properties and fatigue crack growth rate in welded AA-2024," *Materials Science and Engineering*, vol. 779, p. 139116, 2020.

[13] X. Sauvage, A. Dédé, A. C. Muñoz, and B. Huneau, "Precipitate stability and recrystallisation in the weld nuggets of friction stir welded Al-Mg-Si and Al-Mg-Sc alloys," *Materials Science and Engineering*, vol. 491, no. 1-2, pp. 364–371, 2008.

[14] Y. S. Sato, M. Urata, and H. Kokawa, "Parameters controlling microstructure and hardness during friction-stir welding of precipitation-hardenable aluminum alloy 6063," *Metallurgical and Materials Transactions A*, vol. 33, no. 3, pp. 625–635, 2002.

[15] S. V. Sajadifar, G. Moeini, E. Scharifi, C. Lauhoff, S. Böhm, and T. Niendorf, "On the effect of quenching on postweld heat treatment of friction-stir-welded aluminum 7075 alloy," *Journal of Materials Engineering and Performance*, vol. 28, no. 8, pp. 5255–5265, 2019.

[16] K. Elangovan and V. Balasubramanian, "Influences of tool pin profile and welding speed on the formation of friction stir processing zone in AA2219 aluminium alloy," vol. 200, no. 1-3, pp. 163–175, 2008.

[17] R. I. Rodriguez, J. B. Jordon, P. G. Allison, T. Rushing, and L. Garcia, "Microstructure and mechanical properties of dissimilar friction stir welding of 6061-to-7050 aluminum alloys," *Materials & Design*, vol. 83, pp. 60–65, 2015.

[18] J. Chen, S. Li, H. Cong, and Z. Yin, "Microstructure and mechanical behavior of friction stir-welded Sc-modified Al-Zn-Mg alloys made using different base metal tempers," *Journal of Materials Engineering and Performance*, vol. 28, no. 2, pp. 916–925, 2019.

[19] C. S. Paglia, K. V. Jata, and R. G. Buchheit, "The influence of artificial aging on the microstructure, mechanical properties, corrosion, and environmental cracking susceptibility of a 7075 friction-stir-weld," *Materials and Corrosion*, vol. 58, no. 10, pp. 737–750, 2007.

[20] H. Jamshidi Aval, "Microstructure and residual stress distributions in friction stir welding of dissimilar aluminium alloys," *Materials & Design*, vol. 87, pp. 405–413, 2015.

[21] N. Martinez, N. Kumar, R. S. Mishra, and K. J. Doherty, "Effect of tool dimensions and parameters on the microstructure of friction stir welded aluminum 7449 alloy of various thicknesses," *Materials Science and Engineering*, vol. 684, pp. 470–479, 2017.

[22] D. R. Ni, D. L. Chen, B. L. Xiao, D. Wang, and Z. Y. Ma, "Residual stresses and high cycle fatigue properties of friction stir welded SiCp/AA2009 composites," *International Journal of Fatigue*, vol. 55, pp. 64–73, 2013.

[23] R. C. S. Gubbala, "Effect of post weld heat treatment on micro structure & corrosion behavior of aa 7075 friction stir welds," *Defence Technology*, vol. 4, no. 6, pp. 296–299, 2016.

[24] S. J. Andersen, C. D. Marioara, J. Friis, S. Wenner, and R. Holmestad, "Precipitates in aluminium alloys," *Advances in Physics: X*, vol. 3, no. 1, pp. 790–814, 2018.

[25] F. Khodabakhshi, A. Simchi, A. H. Kokabi, and A. P. Gerlich, "Similar and dissimilar friction-stir welding of an PM aluminum-matrix hybrid nanocomposite and commercial pure aluminum: microstructure and mechanical properties," *Materials Science and Engineering*, vol. 666, pp. 225–237, 2016.

[26] S. V. Sujith and R. S. Mulik, "Thermal history analysis and structure-property validation of friction stir welded Al-7079-TiC in-situ metal matrix composites," *Journal of Alloys and Compounds*, vol. 812, p. 152131, 2020.

[27] T. Krol, D. Baither, and E. Nembach, "The formation of precipitate free zones along grain boundaries in a superalloy and the ensuing effects on its plastic deformation," *Acta Materialia*, vol. 52, no. 7, pp. 2095–2108, 2004.

[28] X.-Q. Liu, H.-J. Liu, and Y. Yu, "Relationship between microstructures and microhardness in high-speed friction stir welding of aa6005a-T6 aluminum hollow extrusions," *Acta Metallurgica Sinica*, vol. 33, no. 1, pp. 115–126, 2020.

[29] B. Safarbali, M. Shamanian, and A. Eslami, "Effect of post-weld heat treatment on joint properties of dissimilar friction stir welded 2024-T4 and 7075-T6 aluminum alloys welded 2024-T4 and 7075-T6 aluminum alloys," *Transactions of Nonferrous Metals Society of China*, vol. 28, no. 7, pp. 1287–1297, 2018.

[30] S. D. Ji, X. C. Meng, J. G. Liu, L. G. Zhang, and S. S. Gao, "Formation and mechanical properties of stationary shoulder friction stir welded 6005A-T6 aluminum alloy," *Materials and Design*, vol. 62, pp. 113–117, 2014.

[31] P. V. Kumar, G. M. Reddy, and K. S. Rao, "Microstructure, mechanical and corrosion behavior of high strength AA7075 aluminium alloy friction stir welds - effect of post weld heat treatment," *Defence Technology*, vol. 11, no. 4, pp. 362–369, 2015.

[32] H. Qin, H. Zhang, and H. Wu, "The evolution of precipitation and microstructure in friction stir welded 2195-T8 Al-Li alloy," *Materials Science and Engineering*, vol. 626, pp. 322–329, 2015.

[33] G. Bonny, A. Bakaev, and D. Terentyev, "Assessment of hardening due to non-coherent precipitates in tungsten-rhenium alloys at the atomic scale," *Scientific Reports*, vol. 9, no. 1, pp. 1–10, 2019.

[34] H. K. Pabandi, H. R. Jashnani, and M. Paidar, "Effect of precipitation hardening heat treatment on mechanical and microstructure features of dissimilar friction stir welded AA2024-T6 and AA6061-T6 alloys," *Journal of Manufacturing Processes*, vol. 31, pp. 214–220, 2018.

[35] M. Farahmand Nikoo, H. Azizi, N. Parvin, and H. Yousefpour Naghibi, "The influence of heat treatment on microstructure and wear properties of friction stir welded AA6061-T6/Al2O3 nanocomposite joint at four different traveling speed," *Journal of Manufacturing Processes*, vol. 22, pp. 90–98, 2016.

[36] Z. Y. Ma, R. S. Mishra, and M. W. Mahoney, "Superplastic deformation behaviour of friction stir processed 7075Al alloy," *Acta Materialia*, vol. 50, no. 17, pp. 4419–4430, 2002.

[37] S. Kumar, D. Sethi, S. Choudhury, B. Saha Roy, and S. C. Saha, "An experimental investigation to the influence of traverse speed on microstructure and mechanical properties of friction stir welded AA2050-T84 Al-Cu-Li alloy plates," *Materials Today Proceedings*, vol. 26, no. xxxx, pp. 2062–2068, 2020.

[38] Q. Meng, Y. Liu, J. Kang, R.-d. Fu, X.-y. Guo, and Y.-j. Li, "Effect of precipitate evolution on corrosion behavior of friction stir welded joints of AA2060-T8 alloy," *Transactions of Nonferrous Metals Society of China*, vol. 29, no. 4, pp. 701–709, 2019.

[39] C. Bitondo, U. Prisco, A. Squilace, P. Buonadonna, and G. Dionoro, "Friction-stir welding of AA 2198 butt joints: mechanical characterization of the process and of the welds through DOE analysis," *International Journal of Advanced Manufacturing Technology*, vol. 53, no. 5-8, pp. 505–516, 2011.

[40] D. Trimble, G. E. O'Donnell, and J. Monaghan, "Characterisation of tool shape and rotational speed for increased speed during friction stir welding of AA2024-T3," *Journal of Manufacturing Processes*, vol. 17, pp. 141–150, 2015.

[41] S. Rajakumar, C. Muralidharan, and V. Balasubramanian, "Influence of friction stir welding process and tool parameters on strength properties of AA7075-T6 aluminium alloy joints," *Materials & Design*, vol. 32, no. 2, pp. 535–549, 2011.

[42] M. Kadlec, R. Růžek, and L. Nováková, "Mechanical behaviour of AA 7475 friction stir welds with the kissing bond defect," *International Journal of Fatigue*, vol. 74, pp. 7–19, 2015.

[43] T. Sun, A. P. Reynolds, M. J. Roy, P. J. Withers, and P. B. Prangnell, "The effect of shoulder coupling on the residual stress and hardness distribution in AA7050 friction stir butt welds," *Materials Science and Engineering*, vol. 735, pp. 218–227, 2018.

[44] H. Lin, Y. Wu, and S. Liu, "Impact of initial temper of base metal on microstructure and mechanical properties of friction stir welded AA 7055 alloy," *Materials Characterization*, vol. 146, no. r, pp. 159–168, 2018.

[45] Z. Xie, Z. Jia, K. Xiang et al., "Microstructure evolution and recrystallization resistance of a 7055 alloy fabricated by spray forming technology and by conventional ingot metallurgy," *Metall. Mater. Trans. A Phys. Metall. Mater. Sci.*vol. 51, no. 10, pp. 5378–5388, 2020.

[46] G. Ipekoğlu, S. Erim, and G. Çam, "Effects of temper condition and post weld heat treatment on the microstructure and mechanical properties of friction stir butt-welded AA7075 Al alloy plates," *International Journal of Advanced Manufacturing Technology*, vol. 70, no. 1–4, pp. 201–213, 2014.

[47] E. A. El-Danaf and M. M. El-Rayes, "Microstructure and mechanical properties of friction stir welded 6082 AA in as welded and post weld heat treated conditions," *Materials and Design*, vol. 46, pp. 561–572, 2013.

[48] M. Cabrini, S. Bocchi, G. D'Urso et al., "Effect of Load on the Corrosion Behavior of Friction Stir Welded AA 7075-T6 Aluminum Alloy," *Materials*, vol. 13, p. 2600, 2020.

[49] P. Periyasamy, B. Mohan, and V. Balasubramanian, "Effect of heat input on mechanical and metallurgical properties of friction stir welded AA6061-10% SiCp MMCs," *Journal of Materials Engineering and Performance*, vol. 21, no. 11, pp. 2417–2428, 2012.

[50] P. N. Karakizis, D. I. Pantelis, G. Fourlaris, and P. Tsakiridis, "Effect of SiC and TiC nanoparticle reinforcement on the microstructure, microhardness, and tensile performance of AA6082-T6 friction stir welds," *International Journal of Advanced Manufacturing Technology*, vol. 95, no. 9–12, pp. 3823–3837, 2018.

[51] S. Park, C. G. Lee, H. N. Han, S. J. Kim, and K. Chung, "Improvement of the drawability based on the surface friction stir process of AA5052-H32 automotive sheets," *Metals and Materials International*, vol. 14, no. 1, pp. 47–57, 2008.

[52] S. M. Prabu, H. C. Madhu, C. S. Perugu et al., "Microstructure, mechanical properties and shape memory behaviour of friction stir welded nitinol," *Materials Science and Engineering*, vol. 693, pp. 233–236, 2017.

[53] S. El Mouhri, H. Essoussi, S. Ettaqi, and S. Benayoun, "Relationship between microstructure, residual stress and thermal aspect in friction stir welding of aluminum AA1050," *Procedia Manufacturing*, vol. 32, pp. 889–894, 2019.

[54] P. Sivaraj, D. Kanagarajan, and V. Balasubramanian, "Effect of post weld heat treatment on tensile properties and microstructure characteristics of friction stir welded armour grade AA7075-T651 aluminium alloy," *Def. Technol.*vol. 10, no. 1, pp. 1–8, 2014.

[55] Z. Hao, D. Shaokang, M. Zeming, and W. Jun, "Study on the precipitation behavior of precipitates of 7075 aluminum alloy friction stir welding joint," *Materials Science Forum*, vol. 1003, no. 2, pp. 37–46, 2020.

[56] M. Alipour Behzadi, K. Ranjbar, R. Dehmolaei, and E. Bagherpoour, "Friction-stir-welded overaged 7020-T6 alloy joint: an investigation on the effect of rotational speed on the microstructure and mechanical properties," *Int. J. Miner. Metall. Mater.*vol. 26, no. 5, pp. 622–633, 2019.

[57] W. F. Xu, X. K. Wu, J. Ma, H. J. Lu, and Y. X. Luo, "Abnormal fracture of 7085 high strength aluminum alloy thick plate joint via friction stir welding," *Journal of Materials Research and Technology*, vol. 8, no. 6, pp. 6029–6040, 2019.

[58] J. L. García-Hernández, C. G. Garay-Reyes, I. K. Gómez-Barraza et al., "Influence of plastic deformation and Cu/Mg ratio on the strengthening mechanisms and precipitation behavior of AA2024 aluminum alloys," *Journal of Materials Research and Technology*, vol. 8, no. 6, pp. 5471–5475, 2019.